Available online at www.sciencedirect.com
ScienceDirect
Bioorganic & Medicinal Chemistry 15 (2007) 1420–1429
Bioorganic & Medicinal Chemistry

Molecular modeling of binding between amidinobenzisothiazoles, with antidegenerative activity on cartilage, and matrix metalloproteinase-3

Alessio Amadasi,[a] Pietro Cozzini,[b,*] Matteo Incerti,[c] Elenia Duce,[d] Emilia Fisicaro[d] and Paola Vicini[c]

[a]*Dipartimento di Biochimica e Biologia Molecolare, Via G.P. Usberti 23/A, 43100 Parma, Italy*
[b]*Laboratorio di Modellistica Molecolare, Dipartimento di Chimica Generale ed Inorganica, Chimica Analitica, Chimica Fisica, Via G.P. Usberti 17/A, 43100 Parma, Italy*
[c]*Dipartimento Farmaceutico, Università degli Studi di Parma, Via G.P. Usberti 27/A, 43100 Parma, Italy*
[d]*Dipartimento di Scienze Farmacologiche, Biologiche e Chimiche Applicate, Università degli Studi di Parma, Via G.P. Usberti 27/A, 43100 Parma, Italy*

Received 25 August 2006; revised 25 October 2006; accepted 2 November 2006
Available online 6 November 2006

Abstract—The aim of the work was to investigate the mechanism of binding between human metalloproteinase-3 (MMP-3) and new compounds belonging to the benzisothiazolylamidines class. In vitro tests suggest that these molecules, endowed with antinflammatory and cartilage antidegenerative activity, could act as ligands toward MMP-3. In lack of experimental structural informations, we performed molecular docking simulations to probe the interactions of benzisothiazolylamidines with matrix metalloproteinase-3, using the docking package GOLD and the software HINT as a post-process scoring function. Both GOLD and HINT predicted a binding mode for the compounds under analysis within the hydrophobic S1′ pocket of MMP-3, without interaction with the catalytic Zn^{2+} ion. The scores assigned by the programs to the interaction between the tested benzisothiazolylamidines and human MMP-3 were consistent with a potential direct enzyme inhibitory activity. The highest affinity was predicted for the *N*–(benzo[*d*]isothiazol-3-yl)-4-chlorobenzamidine (**2**), emerged as the most active derivative also in the in vitro tests.

1. Introduction

Matrix metalloproteinases (MMPs) are a superfamily of zinc-containing endopeptidases that mediate the breakdown of extracellular matrix macromolecules like proteoglycans, fibronectin, laminin, and interstitial collagens, associated with tissue destruction in various pathological conditions.[1,2] The proteolytic activities of MMPs are controlled by natural protein inhibitors (mainly tissue inhibitors of metalloproteinases—TIMPs) that act at different levels of the proteolytic cascade of MMP activation.[3,4]

Chronic stimulation of MMP activity could result in a variety of pathological conditions including tumor metastasis,[5] atherosclerosis,[6] neuroinflammation,[7] osteoarthritis (OA), and rheumatoid arthritis.[8–11]

Consequently there is significant interest in the development of drugs to control the aberrant regulation of MMP activity and the worldwide effort on MMP research has led to the discovery of remarkably diverse classes of compounds which are effective inhibitors of MMPs.[12–16]

There is evidence for different pathways for the complex process of metalloproteinase activation and inhibition, but the most common approach in the search for drugs that control abnormal MMP activity is the design of small molecules which bind to the catalytic site of the enzyme. The majority of the MMP inhibitors reported in the literature contain an effective zinc binding group (e.g., hydroxamic acids, carboxylic acids, and sulfhydryl groups), however it was recently demonstrated that non-peptidic inhibitors exhibit hydrophobic binding in the

Keywords: Matrix metalloproteinase-3; Docking; Antiinflammatory; Benzisothiazolylamidines.
* Corresponding author. Tel.: +39 0521 905669; Fax: +39 0521 905556; e-mail: pietro.cozzini@unipr.it

0968-0896/$ - see front matter © 2006 Elsevier Ltd. All rights reserved.
doi:10.1016/j.bmc.2006.11.001

long hydrophobic S1′ pocket yet show no covalent interaction with the catalytic zinc ion.[17,18]

A variety of substrate-based inhibitors have been designed and the features of these effective metalloproteinase inhibitors are well known and extensively reviewed.[15] Concerning the treatment of OA and rheumatoid arthritis, where a shift toward increased MMP activity leads to cartilage degradation and destruction, despite the advances of the medicinal chemistry in this field and the relevance of the related MMP inhibitors, the available chondroprotective agents are still unsatisfactory.[10,19–23]

Indeed, a variety of first-generation MMP inhibitors, designed on the basis of the protein natural substrate, possess peptide-like structure and, on consequence, show poor pharmacokinetic properties. Moreover, the lack of selectivity against a particular subset of the MMPs represents the reason of the unwanted side effects that can cause interruption of clinical trials.[19,20]

Our long-term commitment in the field of benzisothiazole derivatives with biological activity[24–32] led to the discovery of a class of amidinobenzo[*d*]isothiazoles endowed with antinflammatory and antidegenerative activity on cartilage. These compounds, emerged as promising antiinflammatory–antidegenerative agents with non-acidic character, have, in addition, non-peptidic, low weight structures which seem very pertinent properties in the search of new efficient MMP inhibitors.[33,34]

In view of the outstanding in vitro properties shown by the unsubstituted *N*-(benzo[*d*]isothiazol-3-yl)benzamidine and by different substituted benzisothiazolylbenzamidines,[35] we decided to investigate if a direct interaction (i.e., inhibition) of the enzyme, implicated in arthritic diseases,[36,37] with benzisothiazolylamidines may be possible. Indeed, our previous in vitro results showed a powerful reduction, at the micromolar level, of most of the harmful effects induced by the pro-inflammatory cytokine interleukin-1ß on human chondrocytes as detailed by Vicini's paper.[35] The selected amidines for the current study are *N*-(benzo[*d*]isothiazol-3-yl)benzamidine **1**, *N*-(benzo[*d*]isothiazol-3-yl)-4-chlorobenzamidine **2**, emerged as the most active derivative, and *N*-(benzo[*d*]isothiazol-3-yl)acetamidine **3**, considered useful to explain the influence of a different substituent, such as methyl, in the binding process.

The program GOLD was used to perform molecular docking studies, while the software HINT (Hydropatic INTeractions) was used as a post-process scoring function to understand in detail the interactions between protein and synthesized ligands.

GOLD is a well-known automated ligand docking program, that uses a genetic algorithm to explore the full range of ligand conformational flexibility with partial flexibility of the protein side chains.[38,39]

HINT is a non-Newtonian force field, based on experimentally determined Log $P_{o/w}$ (the $\log_{10}$ of the partition coefficient between 1-octanol and water) values, particularly suitable for the quantitative evaluation of non-covalent molecular interactions, including the entropically driven hydrophobic effect,[40–44] therefore, it can constitute a good complementary tool to classical docking software fitness functions.

The method used was found to predict the binding mode of known ligands with good accuracy and then applied to identify the possible binding sites of benzamidines **1**–**3**.

2. Results and discussion

2.1. Selection of the protein target structure

Although GOLD applies some limited flexibility to the protein residue side chains, one of the main problems of any docking analysis lies in the inability in dealing with protein flexibility. Furthermore, human MMP-3 is known to undergo inhibitor-induced conformational changes, with Tyr223 acting as a gatekeeper of the S1′ cavity.[45,46] Because none of the MMP-3 inhibitors reported in the literature exhibits structure similarity with compounds **1**–**3** under study, we decided to compare the crystallographic structures of known MMP-3-ligand complexes, found in the Brookhaven Protein Data Bank, to verify whether differences were present in the position of the binding site residues.

All the complexes were superimposed and a careful analysis was carried out on active site aminoacidic residues (all the residues placed within 4 Å from the position occupied by at least one of the known ligands). With the exception of two complexes, involving non-peptidic thiadiazole inhibitors[45] (PDB code: 1USN and 2USN), rmsd between active site residues (Val163, Leu164, Ala165, His166, Leu197, Val198, His201, Glu202, Glu216, Ala217, Leu218, Met219, Tyr220, Pro221, Leu222, Tyr223, His224, Leu226, and Phe232) of the different MMP-3 complexes are all below 0.75 Å. All the analyzed complexes, with the exception of 1USN and 2USN, exhibit a practically identical active site conformation with the S1′ subsite in the 'open' form. 1USN and 2USN, on the contrary, share an alternative binding site conformation (the rmsd between their active site residues is 0.28 Å) with the S1′ subsite in the 'closed' form, due to a different placement of Tyr223 side chain (see Fig. 1). These findings show that, to date, two alternative conformations of complexed MMP-3 can be found among all known complexes, one exhibiting a S1′ subsite in the 'closed' form and one exhibiting the S1′ subsite in the 'open' form, due to the different behavior of Tyr223 side chain. Other differences between various complexed MMP-3 structures are very little (as shown by the rmsd values) and, mostly, do not seem related to the chemical properties of the different ligands, but are probably due only to the fact that different structures have been solved by different research groups, under different experimental conditions, and with different crystallographic resolution. Therefore, among the crystallographic structures belonging to this two alterna-

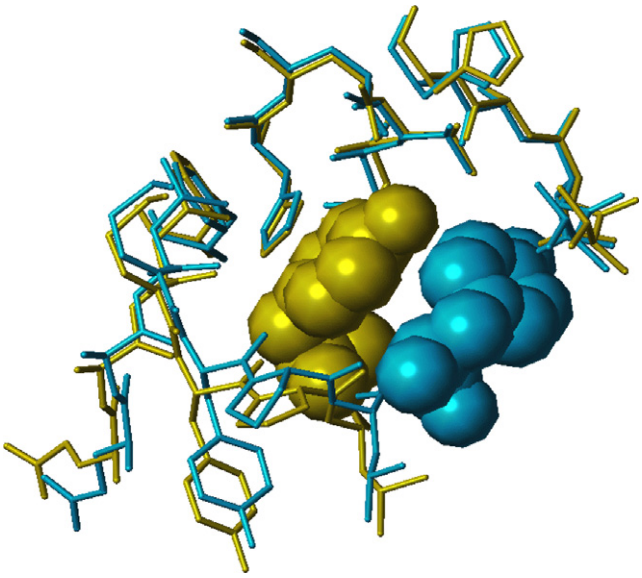

Figure 1. Overlapping of active site residues for the two alternative conformations found among known MMP-3 complexes. The two displayed structures, PDB code: 1CIZ (cyan) and 1USN (yellow), respectively, have been selected as protein targets for docking simulations on benzisothiazolylamidines under study. The different locations of Tyr223, acting as a gatekeeper of the S1′ pocket, are represented in spacefill.

tive conformational classes, the two exhibiting the highest resolution and representative of both the S1′ 'open' and the S1′ 'closed' conformation were selected as protein targets for the docking of the synthesized benzisothiazolylamidines (PDB code 1CIZ (1.6 Å resolution) and 1USN (1.8 Å), respectively). Obviously this choice does not ensure to represent possible different conformational changes, given the significant difference between the structures of amidinobenzisothiazoles and known MMP-3 ligands. However it allows to exploit all the crystallographic evidences, collected to date on human MMP-3 system, to overcome docking program deficiencies in dealing with induce fit.

2.2. Docking studies on known MMP-3 complexes

To assess its reliability, we tested our computational procedure on a dataset of 10 crystallographic complexes between human MMP-3 and inhibitors belonging to different chemical classes (Fig. 2). The structures of all the analyzed complexes, extracted from the Brookhaven Protein Data Bank, were determined at a resolution of 2.5 Å or better to ensure the best performance of the docking algorithms.[38,47] The potency of the inhibitors belonging to the X-ray structures set used varies between 1 and 30 nm (see references in Table 1). The results, obtained using our computational tools to dock the ligand back into the binding site, are shown in Table 1. All the solutions were evaluated on the basis of the rmsd from the experimental orientation. The current standard in the field is a 2.0 Å cut-off, beyond which the prediction is considered a docking failure.[47,55] However, since a small rmsd result may mask a significant error, also a visual inspection of the different solutions was carried out. This subjective analysis confirmed that good solutions on the basis of the rmsd were effectively close to the crystallographically observed binding mode or at least acceptable, that is, showing the displacement of only one ligand group from the experimental structure.

Table 1 confirms that the genetic algorithm is a reliable tool in predicting experimental binding modes[38,39,47] (nine correct poses out of the total ten investigated), while scoring still remains a difficult task. In fact, in only three cases (PDB code: 1BIW, 2USN, and 1G4K) the HINT or GOLD top ranked solution corresponds to the one closest to the experimental orientation. However, considering as satisfactory solutions showing rmsd within 2.0 Å from the crystallographically observed binding mode, we find that GOLD achieves seven correct predictions, while HINT achieves eight correct predictions out of the total ten investigated. Furthermore, the visual inspection revealed that one of the two HINT wrong solutions, relative to the complex between human MMP-3 and a heterocycle-based inhibitor (PDBcode: 1D8M), despite a rmsd of 2.39 Å from the experimental binding mode, could be considered acceptable, because only the hydroxamic group showed a significative displacement from the experimental binding mode, as shown in Figure 3 (the distance between the predicted and crystallographic position of the hydroxyl oxygen is, actually, 2.54 Å). Therefore, the only clear docking failure was found for the complex between MMP-3 and a biphenylylethyl carboxyalkyl dipeptide (PDBcode: 1HFS). Probably the reason of this error lies in the great size and in the high number of rotatable bonds of the examined compound.[47] Furthermore, the presence of a high number of hydrophobic groups does not aid GOLD, because the main driving force of its algorithm is the identification of hydrogen bonding interactions between the ligand and the protein.[38] While GOLD was very reliable in determining the correct position of hydrogen bonding groups and zinc coordinating groups, its difficulty in properly evaluating the hydrophobic interactions constitutes the main reason for the other errors found in the GOLD top ranked poses. The use of HINT as a post-process scoring function can be useful to overcome this problem, as it can be observed for the results relative to the complexes of MMP-3 with a 4-aminoproline derived inhibitor (PDBcode: 1G49), and MMP-3 with the already mentioned heterocycle-based inhibitor (PDBcode: 1D8M), both bearing hydrophobic groups. Indeed, the best GOLD solution for 1D8M exhibits a wrong placement of phenyl and methoxy-phenyl groups. On the other hand, HINT is able to locate these groups near Leu222 hydrophobic side chain and at the entrance of the S1′ hydrophobic subsite (near Tyr223), respectively, where they are found in the crystallographic structure, due to their hydrophobic nature. Discrepancies in the placement of hydrophobic groups are also found in the HINT and GOLD best solutions for the docking of 1G49 complex. The experimentally determined structure exhibits the methyl group near the sulfonamide placed in proximity of Leu222 side chain, while GOLD best solution shows the same group more exposed to the solvent. Furthermore, the best

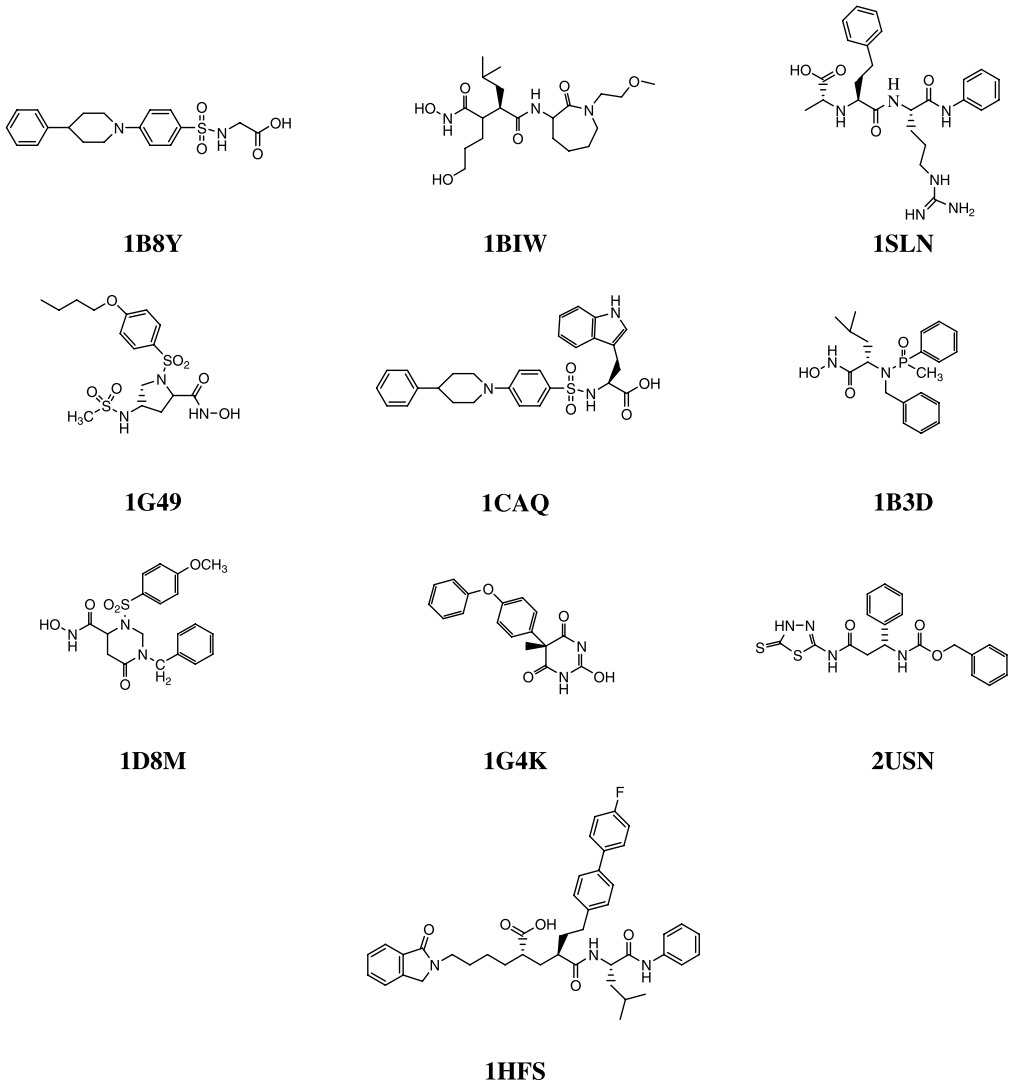

Figure 2. Structures of known inhibitors of human MMP-3. For each ligand the PDB code, relative to the crystallographic structure of the complex formed with stromelysin-1, has been reported.

Table 1. rmsd between computational predictions and experimentally observed binding modes, relative to docking studies carried out on known MMP-3 crystallographic complexes

PDB code	Resolution (Å)	rmsd (Å) best solution[a]	rmsd (Å) GOLD top ranked solution	rmsd (Å) HINT top ranked solution
1CAQ[48]	1.80	0.59	0.63	1.80
1B8Y[48]	2.00	0.62	1.45	1.45
1BIW[49]	2.50	0.74	0.74	1.00
1B3D[46]	2.30	0.79	1.50	1.18
1D8M[50]	2.44	0.79	3.45	2.39
2USN[45]	2.20	0.64	0.64	0.96
1SLN[51]	2.27	1.35	1.81	1.81
1G49[52]	1.90	1.05	4.56	1.65
1G4K[53]	2.00	0.20	0.59	0.20
1HFS[54]	1.70	3.54	11.47	4.57

[a] rmsd between the crystallographic binding mode and the docking solution closest to the crystallographic binding mode.

GOLD owns the alkyloxy chain on the phenyl group near Ala217 and Thr215 hydrophilic carbonyl groups, while both best HINT and the crystallographic complex display this portion of the examined inhibitor within the hydrophobic entrance of the S1′ pocket.

2.3. Docking studies on synthesized benzisothiazolylamidines

The program GOLD was used to dock compounds **1**, **2**, and **3** (Table 2) into the active site of MMP-3 in both S1′

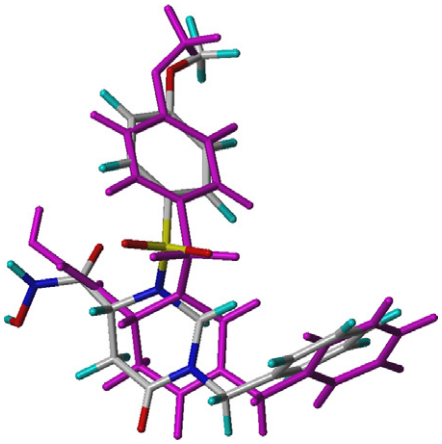

Figure 3. Comparison between the crystallographic binding mode and the docking solution exhibiting the highest HINT score (best HINT in magenta), for the complex between MMP-3 and a heterocycle-based inhibitor (PDBcode: 1D8M).

'closed' (PDB code: 1USN)[45] and S1′ 'open' (PDB code: 1CIZ)[48] conformation (see Fig. 1). For each compound the most stable docking model was selected according to the best scored conformation predicted by GOLD (highest GOLD score) and HINT (highest HINT score).

Being the acid-base properties of the amidino group very sensitive to the substituent in the molecule,[56,57] in order to know what species is present at the physiological pH, it is necessary to carefully evaluate the pK_a of the *N*-benzo[*d*]isothiazol-3-yl-amidines **1**–**3** under investigation: this was done by means of potentiometric titrations in methanol/water = 9:1 as solvent, to avoid solubility problems with the unprotonated form of the hydrochlorides. The values obtained, reported in Table 2, show that, in agreement with the different electronic effects of the substituents, under physiological conditions compounds **1** and **2** are in neutral form, whereas for compound **3** a non-negligible portion of the protonated form is still present.

Compounds **1** and **2** were modeled with the amidino group in the neutral form, in agreement with experimental pK_a of 5.40 and 4.84, respectively, while compound **3**, showing a pK_a of 6.99, was modeled in both the protonated and neutral forms and mean HINT score and GOLD score values have been reported.

The three compounds showed high score values, consistent with a possible binding to MMP-3, only when docked into the S1′ 'open' active site configuration. Significant differences were not found between the binding orientation of the HINT and GOLD predicted best solutions for the synthesized compounds (i.e., the rmsd between HINT and GOLD top ranked solutions was always below 0.70 Å). Furthermore, a cluster analysis performed with a 0.70 Å rmsd tolerance (see Fig. 4) showed a high ratio of conformations very close to the HINT and GOLD best one (85% for compound **2**, 70% for compound **1**, 25% for compound **3** in the protonated form, and 70% for compound **3** in the neutral form). As reported in Table 2, both HINT and GOLD identify the newly synthesized compound **2**, emerged as the most active derivative during in vitro studies[35], as the one which can interact more tightly with human MMP-3, while compound **3** is predicted to have a lower binding affinity. Only for compound **3**, when modeled as protonated, the predicted distance between the benzisothiazol N-atom and Zn^{2+} ion (1.92 Å) is consistent with a possible metal coordination. However the coordination geometry, considering the positions of the three imidazol N-atoms involved in zinc coordination, belonging to His201, His205, and His211, is quite distorted from the tetrahedral one or the trigonal bipiramidal described for other known MMP-3 inhibitors,[48] being the angle between benzoisothiazol N-atom, Zn^{2+} ion, and imidazol N-atom of His205 146.1°. This finding indicates that, probably, also compound **3** cannot undertake a correct metal coordination, but it is located by the software in a position close to the Zn^{2+} ion to allow a strong electrostatic interaction between its positively charged amidino group and the negatively charged carboxylate group of Glu202. However, the absence of available space for the presence of a water molecule allowing the completion of the Zn^{2+} coordination suggests that this predicted binding mode could represent a false positive, due to the high energetic cost associated with this situation. This interpretation is supported by the finding that an alternative docking solution, exhibiting compound **3** into the S1′ pocket (see below), is within a more populated cluster (as shown in Fig. 4c). Therefore, this latter solution, very similar to the one predicted for compound **3** when modeled as deprotonated (see below), can also be considered the more probable binding mode for compound **3** in the protonated form. The likely absence of zinc-coordination, for all the three tested compounds,

Table 2. Structures, experimental pK_a values, HINT calculated Log $P_{o/w}$ values, and best HINT and GOLD score values of the synthesized compounds

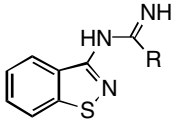

Compound	R	pK_a[a]	Log $P_{o/w}$	Best HINT	Best GOLD
1	C_6H_5	5.40(0.04)	3.52	2397	54.42
2	4-Cl–C_6H_4	4.84(0.01)	4.23	2823	57.60
3	CH_3	6.99(0.01)	2.41	1582	46.42

[a] In MeOH/H_2O = 9:1, I = 0.1 M KCl.

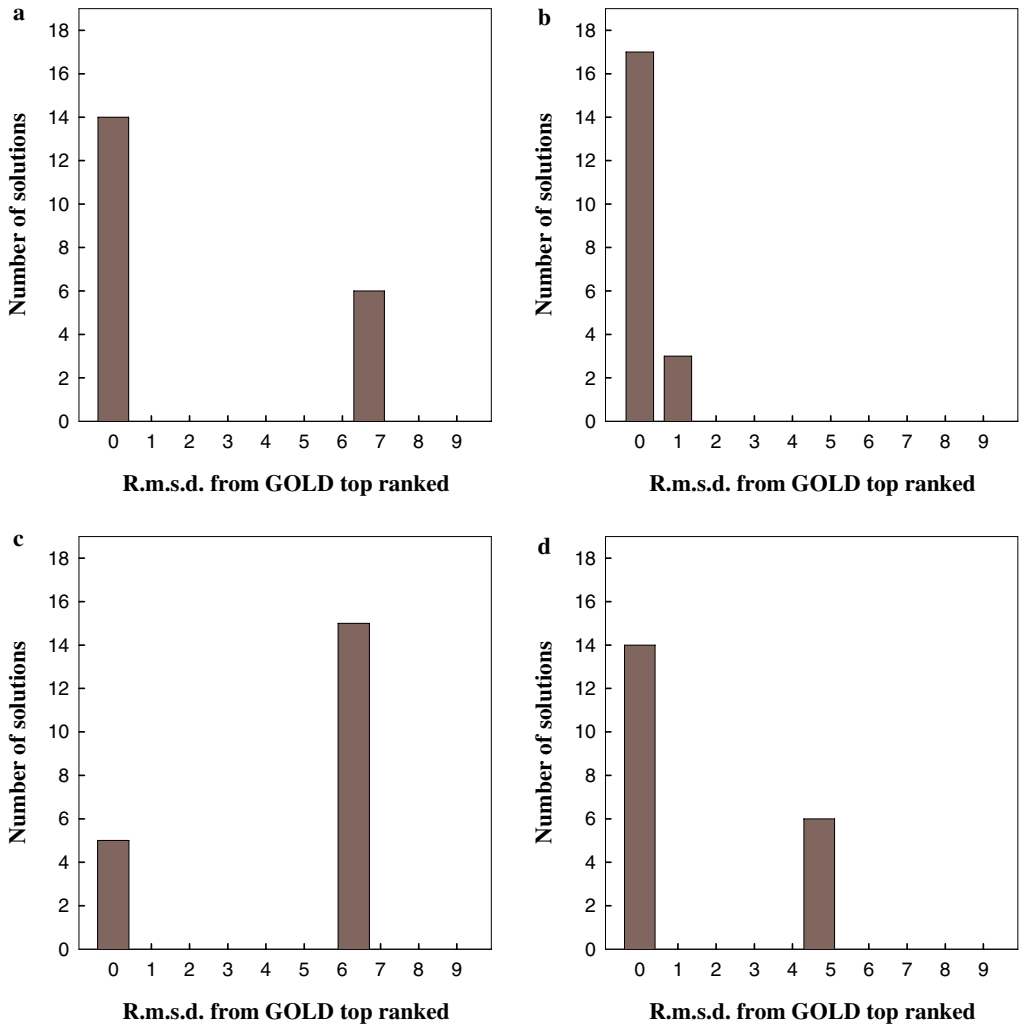

Figure 4. Cluster analysis performed on the 20 docking solutions generated by GOLD for compounds **1** (a), **2** (b) and compound **3** (both protonated (c) and deprotonated (d), with a 0.70 Å rmsd tolerance. On the *x*-axis has been reported the rmsd (Å) of the different clusters from the one including the GOLD top ranked solution (highest GOLD score).

is ascribable to the presence of a steric hindrance in proximity of both the benzisothiazole N-atom and the amidino group, due to a phenyl group and a Cl–phenyl group for **1** and **2**, respectively, and to a methyl group for **3**. The steric clashes between these groups and the protein residues placed in proximity of the zinc atom cannot be overcome by ligand flexibility, given the rigid nature of the tested compounds, thus preventing the N-atom from achieving correct coordination distances and geometries. Actually, both compounds **1** and **2**, as well as compound **3** in the neutral form, are predicted to bind to human MMP-3 within the well-known S1′ subsite[45,48,58] without interactions with the catalytic Zn301 and the highly conserved Glu202. This unusual binding mode for MMP-3 inhibitors does not contrast with knowledge that an intact S1′ substructure is essential for enzyme function,[58] and is in agreement with recent studies concerning a novel series of MMP inhibitors, with low nanomolar affinities, which exhibits extensive hydrophobic binding in the S1′ pocket without interactions with the catalytic zinc ion.[18] The S1′ is a hydrophobic pocket shaped by five leucine residues (Leu164, Leu197, Leu218, Leu222, and Leu226), one valine (Val198), one proline (Pro221), one methionine (Met219), two tyrosine residues (Tyr220, Tyr 223), two histidine residues (His201, His224), and a phenylalanine (Phe232). Two are the regions, within this cleft, showing a particularly hydrophobic character: the first, at the entrance, constituted by the side chains of Leu164, Val198, and Tyr223, the second and more hydrophobic, at the bottom of the cavity, formed by the side chains of Leu197, Leu218, Leu226 and Phe232 (Fig. 5). A more hydrophilic area, shaped mostly by backbone atoms, is located in the middle of the S1′ subsite. Compounds **1** and **2** and compound **3** place their amidino group in this region, allowing hydrogen bond formation with protein main-chain atoms, and leave the benzisothiazole ring and the other hydrophobic substituent into the two hydrophobic pockets, respectively, at the entrance and at the bottom of the cavity. The three ligands own an almost equal binding orientation (Fig. 6) and present a very similar hydrogen bonding network. The amidino group of compound **3** can form hydrogen bonds with the carbonyl oxygen of Ala217 and with the imidazol nitrogen of His224 (Fig. 6a). The predicted hydrogen bonding distances are 2.67 ($O_{(Ala217)}$-imino N) and

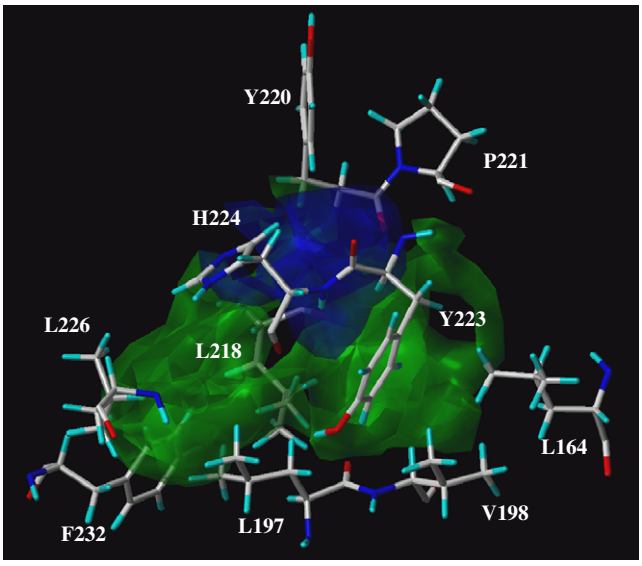

Figure 5. HINT hydrophobic-polar contour map of the S1′ subsite. The 3D contours are spatial representations of the type (color) and strength (contour volume) of the possible interactions. Hydrophobic regions are colored green, while the hydrophilic regions are colored blue. The residues shaping the subsite, rendered in capped sticks, are highlighted.

2.67 ($N_{(His224)}$-imino N). The amidino group of compound **1** can form hydrogen bonds with the carbonyl oxygens of Tyr220 and Leu222, and with imidazol nitrogen of His224 (Fig. 6b). The found hydrogen bonding distances are 2.51 Å ($N_{(His224)}$-imino N), 3.37 Å ($O_{(Tyr220)}$-amidic N) and 3.05 Å ($O_{(Leu222)}$-amidic N). At the same manner the amidino group of compound **2** can undertake hydrogen bonds with the carbonyl oxygens of Tyr220 and Ala217 as well as with the imidazol nitrogen of His224 (Fig. 6c). The predicted hydrogen bonding distances are 3.20 Å ($O_{(Tyr220)}$-amidic N), 2.81 Å ($O_{(Ala217)}$-imino N), and 2.97 Å ($N_{(His224)}$-imino N). In spite of this very similar way of binding, both GOLD and HINT predicted a tighter binding for the last synthesized *p*-Cl-benzamidine derivative than for benzamidine derivative. Being the presence of the *p*-substitution on the phenyl ring the only difference between these two compounds, the only way to rationalize their different affinities for human MMP-3 is mapping the energetics of the interactions between the phenyl and *p*-Cl–phenyl rings and the deeper region of the S1′ subsite, where they are predicted to bind.

In this perspective, to properly investigate the different ability of the three tested compounds in exploiting the hydrophobic character of the S1′ pocket, we analyzed the score values, assigned by HINT, to the interactions undertaken by each ligand with the residues belonging to the two hydrophobic areas of the S1′ subsite. HINT, being based on Log $P_{o/w}$ values derived from a solvation–desolvation experiment, is particularly reliable in the quantitative evaluation of the hydrophobic effects associated with desolvation during ligand binding.[40] Furthermore, this latter investigation is of particular interest, because the S1′ pocket is known to be relevant for achieving potency and selectivity among the MMPs class.[18,48,58] As shown in Table 3, the acetamidine derivative almost does not explore the bottom of the S1′ pocket. This finding suggests a possible poor selectivity of compound **3** for MMP-3.

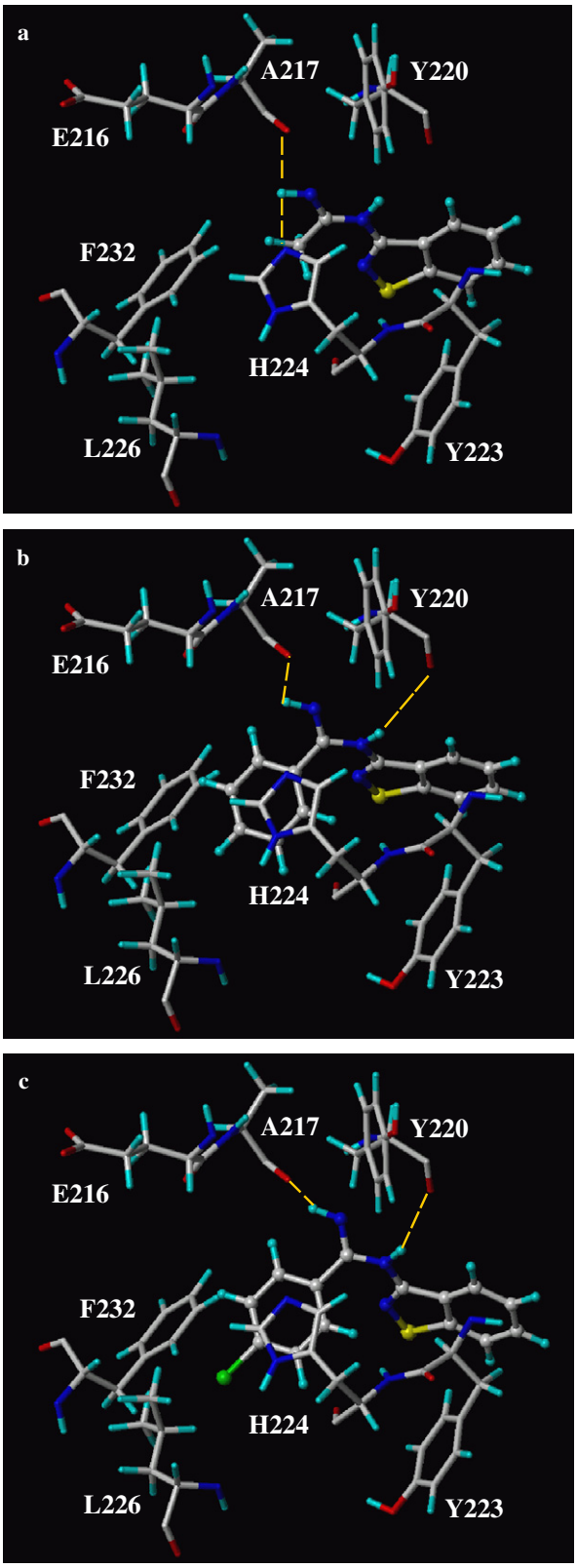

Figure 6. HINT best solution for compounds **1**, **2**, and **3**. Key active site residues are highlighted and yellow lines show possible hydrogen bonds between protein and ligands. (a) Compound **3** modeled in neutral form. (b) Compound **1**. (c) Compound **2**.

Table 3. HINT scores assigned to the interactions between synthesized ligands **1**, **2** and **3** and the residues shaping the two hydrophobic regions at the entrance and at the bottom of the S1′ subsite

Compound	Leu164	Val198	Tyr223	Entrance	Leu197	Leu218	Phe232	Leu226	Bottom
1	13	58	92	163	78	115	29	35	257
2	14	65	84	163	276	113	48	258	695
3	16	53	65	134	−5	13	3	0	11

Compounds **1** and **2** are more able to get advantage from hydrophobic interactions within the S1′ pocket, however, the presence of the Cl-atom, presenting an hydrophobic atomic constant of 0.94, to be compared with a value of 0.23 for an aromatic hydrogen, increases the lipophilicity and the size of compound **2**, improving its ability to energetically explore the bottom of the S1′ pocket and contributing to a great extent to its tighter binding. As it can be seen in Table 3, while the benzamidine and the *p*-Cl-benzamidine derivatives interact in the same manner with the hydrophobic side chains of Leu164, Val198, and Tyr223, located at the entrance of the cavity, the *p*-Cl-benzamidine derivative is able to get a greater advantage from interactions with the highly hydrophobic deeper region and, mostly, with the side chains of Leu197 and Leu226. Actually, HINT assigned a score relative to the interaction with the bottom of the S1′ cavity, of 695 for compound **2**, and of 257 for compound **1**. This finding suggests that the para-substitution with a hydrophobic group of the benzisothiazolylbenzamidine scaffold can increase potency and, probably, selectivity against MMP-3.

3. Conclusions

In absence of more definitive structural data, these models provide our best insight into the understanding of the interaction mechanism between the benzisothiazolylamidines **1**, **2**, and **3**, endowed with antiinflammatory and cartilage antidegenerative activity, and matrix metalloproteinase-3. The combined docking–scoring analysis, carried out using GOLD and HINT, predicted a binding mode for the examined compounds within the hydrophobic S1′ pocket of MMP-3, suggesting a direct competitive enzyme inhibition. These results lead to a better understanding of the benzisothiazolylamidine antiinflammatory–antidegenerative activity and provide guidelines for the design of new MMP-3 inhibitors.

4. Experimental

4.1. Synthesis of *N*-(benzo[*d*]isothiazol-3-yl)amidines

The benzisothiazolylamidines **1**, **2**, and **3** were synthetized using the procedure, previously described by Vicini et al.[24] The complete synthesis, the detailed procedure and the characterization of the compounds are described elsewhere.[24,59]

4.2. Potentiometric measurements

To determine the protonation state of each of the compounds for docking, equilibrium constants for protonation reactions were determined by means of potentiometric measurements (pH $-\log[H^+]$), carried out in methanol/water = 9:1 v/v solution at ionic strength 0.1 mol dm^{-3} KCl and 25 ± 0.1 °C, in the pH range 2.5–10. The titrate concentration varied in the range 5×10^{-3}–7×10^{-3} M. At least two measurements (about 60 experimental points in each) were performed for each system. Titrant solutions were prepared in the same solvent and at the same ionic strength used during measurement. The experimental procedure in order to reach very high accuracy in the determination of the equilibrium constants in mixed solvent has been described in Ref. 60.

Potentiometric titrations were performed by a CRISON GLP 21-22 pHmeter (resolution 0.1 mV) and the titrant was added by means of a Metrohm Dosimat 655 autoburette. Constant-speed magnetic stirring was applied throughout. Sample temperature was controlled to ±0.1 °C by using a circulating water thermostatic bath (ISCO GTR 2000 IIx). 0.1 M KCl in MeOH/H_2O = 9:1 calomel was used as reference electrode (Radiometer Ref. 401). The glass electrode (Crison 5250) was calibrated as hydrogen concentration probe by means of strong acid-strong base titration, by using the Gran's method,[61] allowing the determination of the standard potential E_o (374.5 ± 0.1 mV), and of the ionic product of water in the experimental conditions used, K_w (pK_w = 14.38 ± 0.01).

Both potentiometer and burette were controlled by a home-made program written in BASIC working on IBM computer and allowing that the titrations were automatically performed. The software HYPERQUAD[62] was used to calculate the protonation constants from e.m.f. data.

4.3. Computational studies

The program Sybyl version 6.91 (Tripos, Inc., St. Louis, MO, USA; www.tripos.com), used for this work, was run on a FUEL Silicon Graphics workstation running O.S. IRIX 6.5. The program HINT 3.09 beta test version, not released, was used as an add-on module within Sybyl. This version of HINT has been developed by the authors within a collaboration agreement with Prof. G.E. Kellogg and can be obtained from eduSoft (eduSoft, LC, Ashland, VA, USA; www.edusoft-lc.com). The program GOLD version 2.2 (CCDC, Cambridge, UK; www.ccdc.cam.ac.uk) was installed on a dual pentium processor, with O.S. Linux Red Hat Enterprise 3.0.

4.3.1. Preparation of the protein target and ligands for docking. Three-dimensional coordinates of known protein–ligand complexes were retrieved from the Protein

Data Bank (www.rcsb.org) and imported into the molecular modeling program Sybyl. Structures were checked for correct atom and bond type assignment. Hydrogen atoms, normally not present in the X-ray crystallographic PDB data files, were added using Sybyl Biopolymer and Build/Edit menu tools. Amino-terminal and carboxyl-terminal groups were set to be protonated and deprotonated, respectively. To avoid steric clashes, added hydrogen atoms were energy-minimized using the Powell algorithm, with a gradient of 0.5 kcal $(\text{mol Å})^{-1}$ for 1500 cycles. This procedure affected only not experimentally detected hydrogen atoms.

New synthesized ligands were constructed using the Sketch module of Sybyl and then energy-minimized. Two alternative reference protein coordinates, taken from PDB, were used for the docking of these new ligands: MMP-3 in complex with the thiadiazole inhibitor Pnu-141803 (PDB code: 1USN)[45] and MMP-3 in complex with a non-peptide inhibitor (PDB code: 1CIZ).[48]

4.3.2. Gold. The protein target and the ligands were prepared for docking using Sybyl, as described above and as suggested in previous works.[37] Water molecules and ions, except the zinc ion into the active site, were removed from the PDB structures of the protein target. A radius of 20 Å from the origin was used to direct site location. For each of the genetic algorithm runs, a maximum number of 100,000 operations were performed on a population of 100 individuals with a selection pressure of 1.1. Operator weights for crossover, mutation, and migration were set to 95, 95, and 10, respectively, as recommended by the authors of the software. 20 GA runs were performed in each docking experiment as done in the software validation procedure.[38] The default GOLD fitness function[38] was used to identify the better binding mode. The distance for hydrogen bonding was set to 2.5 Å and the cut-off value for van der Waals calculation was set to 4 Å.

4.3.3. Hydropathic analysis. We used the software HINT (Hydrophatic Interactions) as a post-process scoring function. All the 20 docking poses generated by GOLD for each ligand were re-scored with HINT and the solution exhibiting the highest HINT score (the higher the HINT score the lower the negative predicted ΔG°) was selected as the best docking model for HINT. HINT first calculates $\text{Log}\,P_{\text{o/w}}$ for each component (protein and ligand) of the complex. For proteins the partition method is 'dictionary', where HINT uses a lookup table of parameters based on residue type and solvent condition. The 'neutral' option was chosen as the solvent condition (lysine and arginine were protonated, while glutamic acid and aspartic acid were in the carboxylate form). For the ligands HINT uses the calculate method, an adaptation of the CLOG-P method of Leo.[40] For both protein and ligand the 'essential' option was chosen to perform molecule partition. With this approach only polar hydrogens are treated explicitly. After $\text{Log}\,P_{\text{o/w}}$ calculations, HINT provides a quantitative evaluation of the association process, as a sum of all single atom–atom interactions, using the following equation:

$$\Sigma_i\Sigma_j b_{ij} = \Sigma_i\Sigma_j(a_i S_i a_j S_j T_{ij} R_{ij} + r_{ij})$$

where b_{ij} is the interaction score between atom i and j, a the hydrophobic atomic constant, S the solvent accessible surface area, T_{ij} a logic function assuming +1 or −1 values, depending on the nature of interacting atoms, and R_{ij} and r_{ij} are functions of the distance between atoms i and j.[40]

Acknowledgments

We gratefully acknowledge Prof. D.J. Abraham and Prof. G.E. Kellogg (Virginia Commonwealth University) for the HINT software. HINT was developed in the laboratory of Prof. G.E. Kellogg and can be obtained from eduSoft or Tripos, Inc.

References and notes

1. Skiles, J. W.; Monovich, L. G.; Jeng, A. Y. *Annu. Rep. Med. Chem.* **2000**, *35*, 167.
2. Birkedal-Hansen, H.; Moore, W. G. I.; Bodden, M. K.; Windsor, L. J.; Birkedal-Hansen, B.; De Carlo, A.; Engler, J. A. *Crit. Rev. Oral. Biol. Med.* **1993**, *4*, 197.
3. Belcher, C.; Fawthrop, F.; Bunning, R.; Doherty, M. *Ann. Rheum. Dis.* **1996**, *55*, 230.
4. Woessner, J. F.; Nagase, H. In *Matrix Metalloproteinases and TIMPs*; Oxford University Press, 2000; pp 1–223.
5. Li, M.; Yamamoto, H.; Adachi, Y.; Maruyama, Y.; Shinomura, Y. *Exp. Biol. Med.* **2006**, *231*, 20.
6. Tayebjee, M. H.; Lip, G. Y.; MacFayden, R. J. *Curr. Med. Chem.* **2005**, *12*, 917.
7. Yong, V. W. *Nat. Rev. Neurosci.* **2005**, *6*, 931.
8. Martel-Pelletier, J.; Di Battista, J.; Lajeunesse, D. In *Osteoarthritis: Clinical and Experimental axpects*; Reginster, J.-Y., Martel-Pelletier, J., Pelletier, J. P., Henrotin, Y., Eds.; Springer Berlin: Heidelberg, 1999; pp 156–188.
9. Goldring, M. B. *Arthritis. Rheum.* **2000**, *9*, 1916.
10. Milner, J. M.; Cawston, T. E. *Curr. Drug Targets Inflamm. Allergy* **2005**, *4*, 363.
11. Cawston, T. E. *Mol. Med. Today* **1998**, *3*, 130.
12. Overall, C. M.; Kleifeld, O. *Br. J. Cancer* **2006**, *94*, 941.
13. Radisky, D. C.; Bissell, M. J. *Curr. Opin. Genet. Dev.* **2006**, *16*, 45.
14. Reuben, P. M.; Cheung, H. S. *Front Biosci.* **2006**, *11*, 1199.
15. Kontogiorgis, C. A.; Papaioannou, P.; Hadjipavlou-Litina, D. J. *Curr. Med. Chem.* **2005**, *12*, 339.
16. Ikura, M.; Nakatani, S.; Yamamoto, S.; Habashita, H.; Sugiura, T.; Takahashi, K.; Ogawa, K.; Ohno, H.; Nakai, H.; Toda, M. *Bioorg. Med. Chem.* **2006**, *14*, 4241.
17. Bikádi, Z.; Hazai, E.; Zsila, F.; Lockwood, S. F. *Bioorg. Med. Chem.* **2006**, *14*, 5451.
18. Engel, C. K.; Pirard, B.; Shimanski, S.; Kirsch, R.; Habermann, J.; Klinger, O.; Schlotte, V.; Weithmann, K. U.; Wendt, K. U. *Chem. Biol.* **2005**, *12*, 181.
19. Henrotin, H.; Sanchez, C.; Reginster, J.-Y. *Exp. Opin. Ther. Patents* **2002**, *1*, 29.
20. Hu, Y.; Xiang, J. S.; DiGrandi, M. J.; Du, X.; Ipek, M.; Laakso, L. M.; Li, J.; Li, W.; Rush, T. S.; Schmid, J.; Skotnicki, J. S.; Tam, S.; Thomason, J. R.; Wang, Q.; Levin, J. I. *Bioorg. Med. Chem.* **2005**, *13*, 6629.

21. Whittaker, M.; Floyd, C. D.; Brown, P.; Gearing, J. H. *Chem. Rev.* **1999**, *99*, 2735.
22. Bottomley, K. M.; Johnson, W. H.; Walter, D. S. *J. Enzyme Inhib.* **1998**, *13*, 79.
23. Shröder, J.; Henke, A.; Wenzel, H.; Brandstetter, H.; Stammler, H. G.; Stammler, A.; Pfeiffer, W. D.; Tschesche, H. *J. Med. Chem.* **2001**, *44*, 3231.
24. Vicini, P.; Amoretti, L.; Ballabeni, V.; Barocelli, E.; Chiavarini, M. *Eur. J. Med. Chem.* **1995**, *30*, 809.
25. Vicini, P.; Manotti, C.; Caretta, A.; Amoretti, L. *Arzneim.-Forsch./Drug Res.* **1997**, *47*, 1218.
26. Vicini, P.; Manotti, C.; Caretta, A.; Amoretti, L. *Arzneim.-Forsch./Drug Res.* **1999**, *49*, 896.
27. Vicini, P.; Fisicaro, E.; Lugari, M. T. *Archiv. Pharm. Med. Chem.* **2000**, *333*, 135.
28. Vicini, P.; Amoretti, L.; Ballabeni, V.; Tognolini, M.; Barocelli, E. *Bioorg. Med. Chem.* **2000**, *8*, 2355.
29. Vicini, P.; Zani, F.; Cozzini, P.; Doytchinova, I. *Eur. J. Med. Chem.* **2002**, *37*, 553.
30. Vicini, P.; Geronikaki, A.; Incerti, M.; Busonera, B.; Poni, G.; Cabras, C. A.; La Colla, P. *Bioorg. Med. Chem.* **2003**, *11*, 4785.
31. Geronikaki, A.; Vicini, P.; Theophilidis, G.; Lagunin, A.; Poroikov, V.; Dearden, J. C. *SAR QSAR. Environ. Res.* **2003**, *14*, 485.
32. Zani, F.; Vicini, P.; Incerti, M. *Eur. J. Med. Chem.* **2004**, *39*, 135.
33. Panico, A. M.; Vicini, P.; Incerti, M.; Cardile, V.; Gentile, B.; Ronsisvalle, G. *Il Farmaco* **2002**, *57*, 671.
34. Panico, A. M.; Vicini, P.; Massimo, G.; Cardile, V.; Gentile, B.; Avondo, S.; Vittorio, F.; Ronsisvalle, G. *Inflammation* **2004**, *28*, 231.
35. Vicini, P.; Incerti, M.; Cardile, V.; Garufi, F.; Ronsisvalle, S.; Panico, A.M. *Chem. Med. Chem.*, in press.
36. Okada, Y.; Takeuchi, N.; Tomita, K.; Nakanishi, I.; Nagase, H. *Ann. Rheum. Dis.* **1989**, *48*, 645.
37. Obata, K.; Iwata, K.; Okada, Y.; Kohrin, Y.; Ohuchi, E.; Yoshida, S.; Shinmei, M.; Hayakawa, T. *Clin. Chim. Acta* **1992**, *211*, 59.
38. Jones, G.; Willett, P.; Glen, R. C.; Leach, A. R.; Taylor, R. *J. Mol. Biol.* **1997**, *267*, 727.
39. Verdonk, M. L.; Cole, J. C.; Hartshorn, M. J.; Murray, C. W.; Taylor, R. D. *Proteins: Struct., Funct., Genet.* **2003**, *52*, 609.
40. Kellogg, G. E.; Burnett, J. C.; Abraham, D. J. *J. Comput.-Aided Mol. Des.* **2001**, *15*, 381.
41. Abraham, D. J.; Kellogg, G. E.; Holt, J. M.; Ackers, G. K. *J. Mol. Biol.* **1997**, *272*, 613.
42. Cozzini, P.; Fornabaio, M.; Marabotti, A.; Abraham, D. J.; Kellogg, G. E.; Mozzarelli, A. *J. Med. Chem.* **2002**, *45*, 2469.
43. Spyrakis, F.; Fornabaio, M.; Cozzini, P.; Mozzarelli, A.; Abraham, D. J.; Kellogg, G. E. *J. Am. Chem. Soc.* **2004**, *126*, 11764.
44. Wang, R.; Lu, Y.; Fang, X.; Wang, S. *J. Chem. Inf. Comput. Sci.* **2004**, *44*, 2114.
45. Finzel, B. C.; Baldwin, E. T.; Bryant, G. L.; Hess, G. F.; Wilks, J. W.; Trepod, C. M.; Mott, J. E.; Marshall, V. P.; Petzold, G. L.; Poorman, R. A.; O'Sullivan, T. J.; Schostarez, H. J.; Mitchell, M. A. *Protein Sci.* **1998**, *7*, 2118.
46. Chen, L.; Rydel, T. J.; Gu, F.; Dunaway, C. M.; Pikul, S.; Dunham, K. M.; Barnett, B. L. *J. Mol. Biol.* **1999**, *293*, 545.
47. Kontoyianni, M.; McClellan, L. M.; Sokol, G. S. *J. Med. Chem.* **2004**, *47*, 558.
48. Pavlovsky, A. G.; Williams, M. G.; Ye, Q.-Z.; Ortwine, D. F.; Purchase, C. F.; White, A. D.; Dhanaraj, V.; Roth, B. D.; Johnson, L. L.; Hupe, D.; Humblet, C.; Blundell, T. L. *Protein Sci.* **1999**, *8*, 1455.
49. Natchus, M. G.; Cheng, M.; Wahl, C. T.; Pikul, S.; Almstead, N. G.; Bradley, R. S.; Taiwo, Y. O.; Mieling, G. E.; Dunaway, C. M.; Snider, C. E.; McIver, J. M.; Barnett, B. L.; McPhail, S. J.; Anastasio, M. B.; De, B. *Bioorg. Med. Chem. Lett.* **1998**, *8*, 2077.
50. Pikul, S.; Dunham, K. M.; Almstead, N. G.; De, B.; Natchus, M. G.; Taiwo, Y. O.; Williams, L. E.; Hynd, B. A.; Hsieh, L. C.; Janusz, M. J.; Gu, F.; Mieling, G. E. *Bioorg. Med. Chem. Lett.* **2001**, *11*, 1009.
51. Becker, J. W.; Marcy, A. I.; Rokosz, L. L.; Axel, M. G.; Burbaum, J. J.; Fitzgerald, P. M. D.; Cameron, P. M.; Esser, C. K.; Hagmann, W. K.; Hermes, J. D.; Springer, J. P. *Protein Sci.* **1995**, *4*, 1966.
52. Natchus, M. G.; Bookland, R. G.; De, B.; Almstead, N. G.; Pikul, S.; Janusz, M. J.; Heitmeyer, S. A.; Hookfin, E. B.; Hsieh, L. C.; Dowty, M. E.; Dietsch, C. R.; Patel, V. S.; Garver, S. M.; Gu, F.; Pokross, M. E.; Mieling, G. E.; Baker, T. R.; Foltz, D. J.; Peng, S. X.; Bornes, D. M.; Strojnowski, M. J.; Taiwo, Y. O. *J. Med. Chem.* **2000**, *43*, 4948.
53. Dunten, P.; Kammlott, U.; Crowther, R.; Levin, W.; Foley, L. H.; Wang, P.; Palermo, R. *Protein Sci.* **2001**, *10*, 923.
54. Esser, C. K.; Bugianesi, R. L.; Caldwell, C. G.; Chapman, K. T.; Durette, P. L.; Girotra, N. N.; Kopka, I. E.; Lanza, T. J.; Levorse, D. A.; MacCoss, M.; Owens, K. A.; Ponpipom, M. M.; Simeone, J. P.; Harrison, R. K.; Niedzwiecki, L.; Becker, J. W.; Marcy, A. I.; Axel, M. G.; Christen, A. J.; McDonnell, J.; Moore, V. L.; Olszewski, J. M.; Saphos, C.; Visco, D. M.; Shen, F.; Colletti, A.; Krieter, P. A.; Hagmann, W. K. *J. Med. Chem.* **1997**, *40*, 1026.
55. Brooijmans, N.; Kuntz, I. D. *Annu. Rev. Biophys. Biomol. Srtuct.* **2003**, *32*, 335.
56. Oszczapowicz, J.; Jaroszewska-Manaj, J.; Golimowska, K. *J. Chem. Soc., Perkin Trans. 2* **2000**, 2343.
57. Greenhill, J. V. *J. Chem. Soc., Perkin Trans. 2* **1985**, 1255.
58. Johnson, L. L.; Pavlovsky, A. G.; Johnson, A. R.; Janowicz, J. A.; Man, C-F.; Ortwine, D. F.; Purchase, C. F., II; White, A. D.; Hupe, D. J. *J. Biol. Chem.* **2000**, *275*, 11026.
59. Vicini, P.; Zani, F. *Il Farmaco* **1997**, *52*, 21.
60. Fisicaro, E.; Braibanti, A. *Talanta* **1988**, *10*, 769.
61. Gran, G. *Analyst (London)* **1952**, *77*, 661.
62. Gans, P.; Sabatini, A.; Vacca, A. *Talanta* **1996**, *43*, 1739.